Electronic Supplementary Material (ESI) for ChemComm.

Encapsulation induced aggregation – A self-assembly strategy for weakly pi-stacking chromophores

Soumik Sao, Ishita Mukherjee, Priyadarsi De and Debangshu Chaudhuri*

Department of Chemical Sciences and Centre for Advanced Functional Materials (CAFM)

Indian Institute of Science Education and Research (IISER) Kolkata, Mohanpur 741246, India

Email: dchaudhuri@iiserkol.ac.in

Table of Contents

I. Materials and methods

All reagents, solvents (GR and spectroscopic grade) were bought from Sigma–Aldrich and used as received, unless specified. Methyl methacrylate (MMA, 99%) and poly(ethylene glycol) methyl ether methacrylate (PEGMA, molecular weight 300 g/mol, 99%) were purified through a basic alumina column prior to polymerization. The 2,2′-azobisisobutyronitrile (AIBN, 98%) radical initiator was recrystallized twice from methanol. $CDCl_3$ (99.8% D) was purchased from Cambridge Isotope Laboratories, Inc., USA for NMR study. The synthesis of 4-cyano-4-(dodecylsulfanylthiocarbonyl) sulfanylpentanoic acid (CDP) was conducted according to an earlier reported procedure[1]. The solvents such as hexanes (mixture of isomers), tetrahydrofuran (THF), acetone, were purified by standard procedures. Column chromatography was performed on silica gel (100– 200 mesh). TLC analyses were performed on aluminum plates coated with Merck silica gel 60 F254 and visualization under UV light (254 and 365 nm).

Gel permeation chromatography (GPC) measurements were conducted in THF at 30 ^{o}C with a flow rate of 1.0 mL/min (equipped with a Waters Model 515 HPLC pump, two PolarGel-M analytical columns (300 × 7.5 mm)). Detection consisted of Waters Model 2414 refractive index (RI) detector. Narrow molecular weight poly(methyl methacrylate) (PMMA) standards were used to calibrate the system. NMR spectra were acquired in a Bruker Avance^{III} 500 MHz spectrometer. Size distributions were determined using a dynamic light scattering (DLS) (Zetasizer Nano ZS, Malvern Instrument Ltd., UK) instrument equipped with a He–Ne laser beam at 658 nm. Polymer solutions were filtered through a 0.45 μm syringe filter prior to analysis and each experiment was repeated at least three times to obtain the average value. Field emission scanning electron microscopy (FE-SEM) samples were prepared as follows: an aliquot of sample solution was drop casted on a silicon wafer, vacuum dried, coated with gold:palladium (20:80) alloy. Finally, images were recorded using a Carl Zeiss-Sigma instrument. Samples for transmission electron microscopy (TEM) were prepared by drop-casting aqueous suspension of polymer micelles on carbon coated Cu grid followed by air drying.TEM was performed on JEOL JEM-1400 Plus, operated at 120 KV. Optical absorption spectroscopy was performed on a Perkin-Elmer Lambda 35 spectrophotometer and samples were analyzed in quartz cuvette of 1 cm path length. Fluorescence spectra were recorded on Perkin Elmer LS 55 Luminescence spectrometer and samples were analyzed in quartz cuvette of 1 cm path length.

II. Syntheses and characterization

RAFT polymerization of MMA

MMA was polymerised *via* RAFT technique in of *N*, *N*'-dimethylformamide (DMF) at 70 °C using AIBN as radical initiator and CDP as CTA (Scheme 1) using two different [MMA]/[CDP] ratios (Table 1), at 10% AIBN to CDP ratio to obtain polymers with controlled molecular weight, narrow dispersity (*Đ*) and defined chain ends. A typical polymerization procedure is described as follows: MMA (3.0 g, 29.96 mmol), CDP (161.20 mg, 0.39 mmol), AIBN (6.56 mg, 39.95 µmol) and 10.0 g of DMF were added to a 20 mL septa sealed glass vial equipped with a magnetic bar and purged under dry N_2 gas for 15 min. The reaction vial was placed in a preheated reaction block at 70 °C for 5 h, after which the polymerization reaction was quenched by cooling the vial in an ice-water bath. The polymer was purified from acetone solutions by reprecipitation in hexanes at least five times, and dried under high vacuum at room temperature for 12 h. The GPC RI traces for both the homopolymers indicate unimodal distribution (Fig. S1). Number average molecular weights ($M_{n,GPC}$) and *Đ* values were determined from GPC analysis (Table 1). Theoretical number average molecular weight ($M_{n,theo}$) was obtained from the gravimetric conversion data. PMMA was characterized by ^{1}H NMR spectroscopy in$CDCl_3$ (Fig. S2). Typical resonance signals for the different protons in the repeating unit of the polymer are assigned on the spectrum. From the NMR chain-end analysis, the molecular weights ($M_{n,NMR}$) were determined. Good agreement between $M_{n,GPC}$, $M_{n,theo}$, $M_{n,NMR}$ suggests controlled RAFT polymerization (Table 1).

Syntheses and characterization of block copolymers

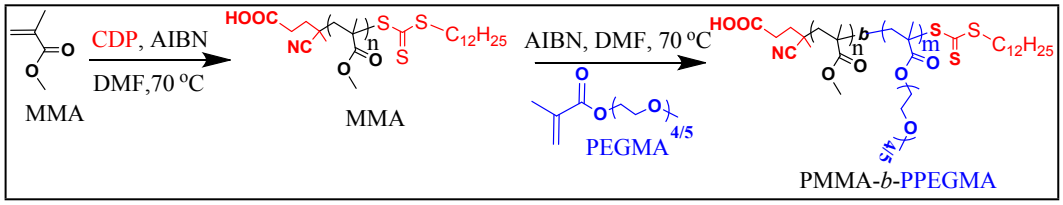

Scheme 1 Synthesis of PMMA homopolymer, corresponding PMMA-*b*-PPEGMA di-block copolymers via RAFT polymerization

A typical block copolymerization protocol is described as follows: PEGMA (1.0 g, 3.33 mmol), PMMA macro-CTA ($M_{n,GPC}$ = 4200 g/mol, *Đ* = 1.12, 294 mg, 0.07 mmol), AIBN (1.15 mg, 7.0 µmol), and DMF (4.0 g) were taken in a 20 mL polymerization vial equipped with a magnetic bar and purged under dry N_2 gas for 15 min. The reaction vial was put in a preheated reaction block at 70 °C for 6.5 h. The resulting block copolymer, PMMA-*b*-PPEGMA, was purified as mentioned above for the homopolymer. MMA was polymerised *via* RAFT technique in DMF at 70 °C using AIBN as radical initiator and CDP as CTA (Scheme

1) using two different [MMA]/[CDP] ratios (Table 1), at 10% AIBN to CDP ratio to obtain polymers with controlled molecular weight, narrow dispersity (*Đ*) (1.12-1.23) and defined chain ends. The GPC RI traces for both the homopolymers indicate unimodal distribution (Figure S1). Number average molecular weights ($M_{n,GPC}$) and *Đ* values were determined from GPC analysis (Table 1). Theoretical number average molecular weight ($M_{n,theo}$) was obtained from the gravimetric conversion data. PMMA was characterized by ^{1}H NMR spectroscopy in $CDCl_3$ (Figure S2). Typical resonance signals for the different protons in the repeating unit of the polymer are assigned on the spectrum. From the NMR chain-end analysis, the molecular weights ($M_{n,NMR}$) were determined. Good agreement between $M_{n,GPC}$, $M_{n,theo}$, $M_{n,NMR}$ suggests controlled RAFT polymerization (Table 1).

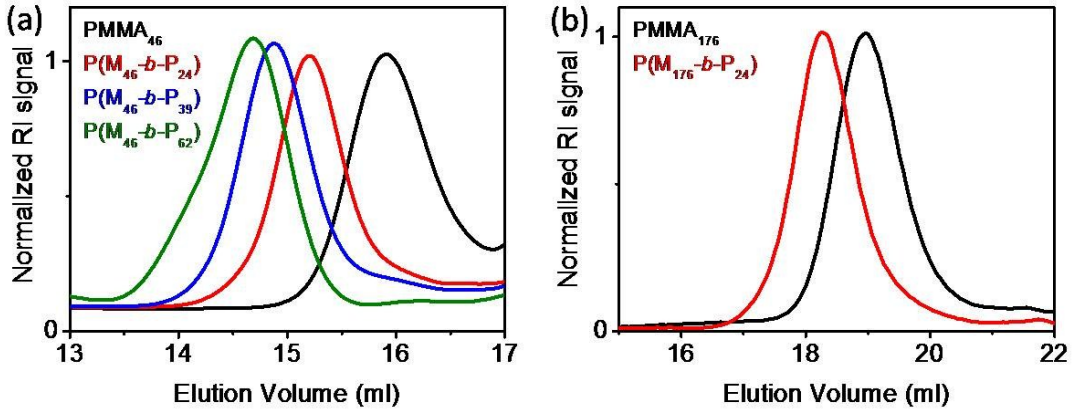

Fig. S1 The GPC RI traces of the PMMA-macroCTA and P(M-*b*-P) block copolymers

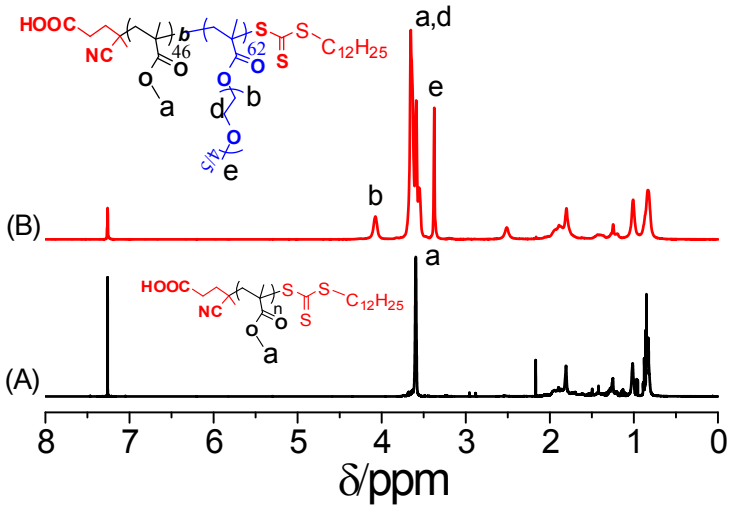

Fig. S2 ^{1}H NMR spectra in $CDCl_3$ of (A) $PMMA_{46}$ and (B) $P(M_{46}$-*b*-$P_{62})$ block copolymer

Polymers	Ratio [Monomer]/[CTA]/[AIBN]	Time (h)	Conv. (%)[e]	$M_{n,GPC}$[f] (g mol^{-1})	$Đ$[f]	$M_{n,NMR}$[g] (g mol^{-1})	$M_{n,theo}$[h] (g mol^{-1})
$PMMA_{46}$[a]	75:1:0.1	5.0	55	4200	1.12	5000	4500
$PMMA_{176}$[b]	240:1:0.1	6.0	55	17300	1.11	18000	13600
$P(M_{46}$-*b*-$P_{24})$[c]	25:1:0.1	6.0	89	7000	1.14	12100	11600
$P(M_{46}$-*b*-$P_{39})$[c]	50:1:0.1	6.5	76	9000	1.18	16800	16400
$P(M_{46}$-*b*-$P_{62})$[c]	75:1:0.1	7.0	83	12400	1.16	23700	23600
$P(M_{46}$-*b*-$P_{85})$[c]	110:1:0.1	8.0	86	16000	1.23	30400	33300
$P(M_{176}$-*b*-$P_{24})$[d]	110:1:0.1	7.0	78	22800	1.13	25200	43700

Table 1 RAFT synthesis of PMMA and block copolymers in DMF at 70 °C

[a,b][Monomer]/[CTA]/[AIBN] = [MMA]/[CDP]/[AIBN]. [c][Monomer]/[CTA]/[AIBN] = [PEGMA]/[PMMA[a]]/[AIBN]. [d][Monomer]/[CTA]/[AIBN] = [PEGMA]/[PMMA[b]]/[AIBN]. [e]Conversion as determined gravimetrically on the basis of the amount of monomer feed. [f]Measured by GPC. [g]Calculated by ^{1}H NMR spectroscopy. [h]$M_{n,theo}$ = (([monomer]/[CTA] × average molecular weight (MW) of monomer × conversion) + (MW of CTA)).

In the next stage, five different PMMA-*b*-PPEGMA block copolymers, with variable block lengths of PPEGMA were synthesized using PMMA macro-CTA with different ratios 0f [PEGMA]/[PMMA macro-CTA] and a fixed ratio of [PMMA macro-CTA]:[AIBN] = 1:0.1. Results are shown in Table 1, where block copolymers were named as follows: M = PMMA segment and P = PPEGMA segment. Degree of polymerization (*DP*) of each block is denoted by the subscripts after each block abbreviation; for example, $P(M_{46}$-*b*-$P_{24})$ represents the PMMA-*b*-PPEGMA block copolymer which consists of a PMMA block of *DP* = 46 and PPEGMA block of *DP* = 24. Unimodal GPC RI traces of block copolymers towards higher molecular weight (lower elution volume) was shown with increasing block length (Figure S1). The block copolymers were also characterized by ^{1}H NMR spectroscopy in $CDCl_3$ (Figure S2). $M_{n,GPC}$, $Đ$, $M_{n,theo}$ of all block copolymers are presented in Table 1. $M_{n,NMR}$ determined from NMR chain-end analysis matches well with $M_{n,theo}$.

Syntheses and characterization of dyes

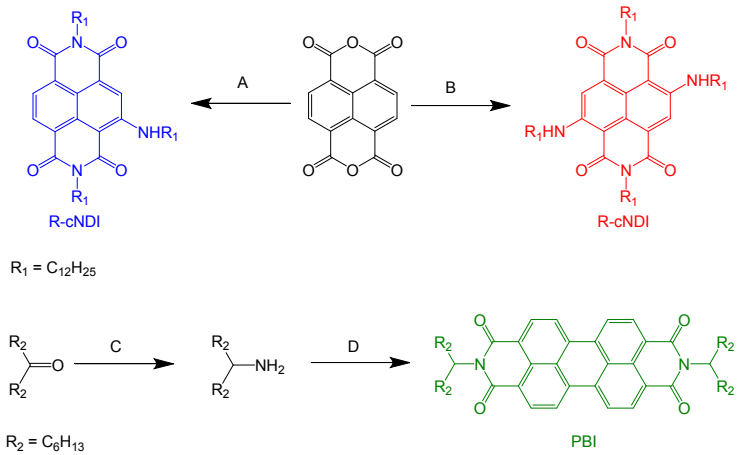

Scheme 2 **A**(i) 5,5-dimethyl-1,3-dibromohydantoin, H_2SO_4, 12 h (ii) $NH_2C_{12}H_{25}$, AcOH, reflux, 3 h (iii) $NH_2C_{12}H_{25}$, dioxane, reflux, 3 h. **B**(i) 5,5-dimethyl-1,3-dibromohydantoin, H_2SO_4, 10 h (ii) $NH_2C_{12}H_{25}$, AcOH, reflux, 4 h (iii) $NH_2C_{12}H_{25}$, dioxane, reflux, 12 h. **C**. $NaCNBH_3$, dry methanol, 30 °C, 12 h. **D**. perylene-3,4,9,10,-tetracarboxylicdianhydride, imidazole, 130 °C, Ar.

(a) R-cNDI

R-cNDI was synthesized done by a known literature procedure with little modification**.** In single necked round bottom flask naphthalene1, 4, 5, 8 -tetracarboxylic dianhydride (NDA, 10 mmol) was stirred in concentrated H_2SO_4 (25 mL) at ambient temperature to obtain a blackish slurry. To this resulting mixture 5,5-dimethyl-1,3-dibromohydantoin (DBH , 5.5 mmol) was added in portions with a duration of 1 h and allowed to stir at room temperature for 12 h to obtain mono-brominated NDA. Then the reaction mixture was poured into crushed ice and the precipitated solid was filtered, washed with water followed by methanol. Next the resulting mixture was taken in a 100 mL round bottom flask and refluxed for 3 h in presence of n-dodecylamine (30 mmol) and 75 mL of acetic acid for 3 h to obtain corresponding imide. After that, the resulting reaction mixture was cooled to allow full precipitation followed by decanting of supernatant solvent. To remove the traces of solvent and amine; the mixture was washed thoroughly with methanol, water and finally with 3 mL of acetone .Next the precipitate was allowed to get dry under high vacuum. Thus obtained dry powder; was further subjected to reflux in dioxane (25 mL) with dodecyl amine (12.5 mmol) for 3 h to form mixture of bay substituted NDIs .Then after removal of solvent under high vacuum , the reaction mixture was purified using column chromatography to obtain red colored R-cNDI in 80 % yield. ^{1}H NMR (500 MHz, $CDCl_3$): δ (ppm). 10.06 (t, 1H, N–H), 8.56–

8.54 (d, J = 8 Hz, 1H, Ar-H), 8.25–8.23 (d, J = 8 Hz, 1H, Ar-H), 8.22 (s, 1H, Ar-H), 4.18–4.13 (m, 4H, $2CH_2$), 3.55–3.51 (q, J = 6.8 Hz, 2H, CH_2), 1.83–1.79 (quin, J = 7.2 Hz, 2H, CH_2), 1.75–1.68 (quin, J = 7.2 Hz, 4H, $2CH_2$), 1.49–1.23 (m, 54H, $27CH_2$), 0.89–0.85 (m, 9H, 3CH3); ^{13}C NMR (125 MHz, $CDCl_3$) δ (ppm) : 166.10, 162.90, 152.23, 131.15, 129.36, 127.80 126.04, 124.28, 123.44, 119.67, 119.23, 99.65, 43.34, 40.88, 40.38,31.90, 29.62, 29.33 27.02,27.08,27.20,28.06,20.6, 22.66, 14.08. MS (ESI-MS) for $[MH]^+$, 787.1879 (calc.), 787.1874 (found). Elemental analysis, found: C, 76.67; H, 10.11; N, 5.33. Calc. for $C_{50}H_{79}N_3O_4$: C, 76.39; H, 10.13; N, 5.34 %.

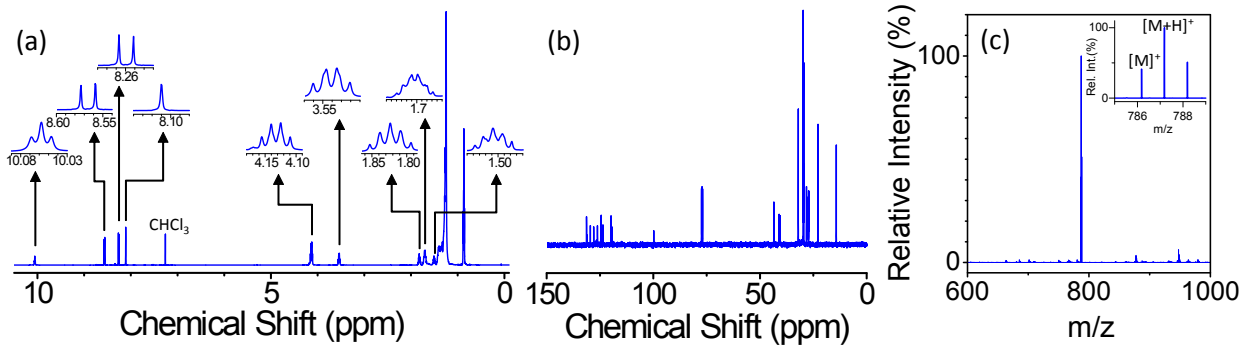

Fig. S3 Characterization of R-cNDI (a) ^1H NMR (b) ^{13}C NMR (c) mass spectra (ESI-MS)

(b) 2R-cNDI

In single neck round bottom flasks naphthalene-1,4,5,8 -tetracarboxylicdianhydride (NDA, 10 mmol) was stirred in concentrated H_2SO_4 (25 mL) at ambient temperature to obtain a blackish slurry. To this resulting mixture 5,5-dimethyl-1,3-dibromohydantoin (DBH) (11 mmole) was added in portions with a duration of 1 h and allowed to stir at room temperature for 10 h to obtain di-brominated NDAs. Then the reaction mixture was poured into crushed ice and the precipitated solid was filtered, washed with water followed by methanol. Next the resulting mixture was taken in a 100 mL round bottom flask and refluxed for 4 h in presence of n-dodecylamine (30 mmole) and 75 mL of acetic acid to obtain corresponding imide .After that, the resulting reaction mixture was cooled to allow full precipitation followed by decanting of supernatant solvent. To remove the traces of solvent and amine the mixture was washed thoroughly with methanol, water and finally with 3 mL of acetone .Next the precipitate was allowed to get dry under high vacuum. Thus obtained dry powder; was further subjected to reflux in dioxane (25 mL) with dodecyl amine (25 mmol) for 12 h to form mixture of bay substituted NDI's .Then after removal of solvent under high vacuum , the reaction mixture was purified using column chromatography to obtain blue colored 2R-cNDI in 90 % yield. ^1H NMR (500 MHz, $CDCl_3$): δ (ppm) 9.33-

9.30 (bs, 2H, N–H), 8.06 (s, 2H, Ar-H), 4.18–4.14 (t, J = 8 Hz, 4H, $2CH_2$), 3.46 (t, J = 6.8 Hz, 4H, $2CH_2$), 1.82–1.78 (quin, J = 7.2 Hz, 4H, $2CH_2$), 1.74–1.66 (m, 4H, $2CH_2$), 1.52–1.48 (m, 4H, $2CH_2$), 1.39–1.17 (m, 72H, $36CH_2$ 0.89–0.86 (m, 12H, $4CH_3$); ^{13}C NMR (125 MHz, $CDCl_3$) δ (ppm) : 166.11, 162.96, 148.97, 125.68, 121.07, 118.3, 101.83, 43.33, 40.46, 31.92, 31.43, 29.35,28.12,21.75 20.6, 22.69, 14.10. MS (ESI-MS) for $[MH]^+$, 970.5215 (calc.), 970.521 (found). Elemental analysis: Found: C, 76.75; H, 10.79; N, 5.76 %. Calc. for $C_{62}H_{104}N_4O_4$: C, 76.81; H, 10.81; N, 5.78 %.

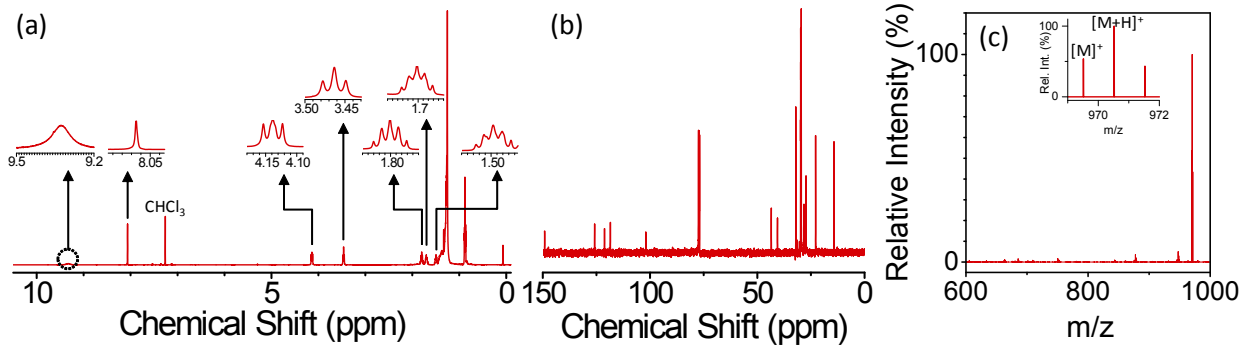

Fig. S4 Characterization of 2R-cNDI (a) ^1H NMR (b) ^{13}C NMR (c) mass spectra (ESI-MS)

(c) PBI

Synthesis of PBI was done by a known literature procedure with little modification[3]**.** In a 250 mL round bottom flux 2.50g (12.6 mmol) 7-tridecanone, 10.0g (129 mmol) NH_4OAc, and 0.56g (8.9 mmol) $NaCNBH_3$ were dissolved in 40 mL dry MeOH and stirred at 30°C for 12 h. The progress of the reaction was monitored by using TLC. Then the reaction was terminated by added concentrated HCl drop wise (~2 mL) then concentrated with a rotary evaporator. The resulting white solid was taken in to 200 mL H_2O, then solid KOH was added to adjust the pH~10 to the mixture, and extracted with 200 mL $CHCl_3$ for three times. The $CHCl_3$ was concentrated to give 2.2 g (86%) of pale yellow oil. In next step this amine was used without any purification. Next in a 250 mL round bottom flask 1.2 g (3.0 mmol) perylene-3,4,9,10-tetracarboxylicdianhydride and 2.6 g (9.3 mmol) and the amine were taken in 6.0g imidazole were warmed at 130°C for 3 h, under argon atmosphere then cooled to room temperature. The reaction mixture was taken up in 100 mL ethanol, treated with 300 mL 2M HCl and stirred overnight. The resulting dark red precipitate was passed in to the filter paper and washed thoroughly with distilled water and dried in vacuum oven at 50°C to yield 2.51g (90%) of red solid. ^1H NMR (500 MHz, $CDCl_3$): δ (ppm) 0.83 (t, 12H), 1.20- 1.30(m, 32H), 1.87(m, 4H), 2.25(m, 4H), 5.18(m, 2H) , 8.67(m, 8H). ^{13}C NMR (125 MHz, $CDCl_3$) δ (ppm) : 164.63, 163.55, 134.49, 131.11,131.86. 129.58, 126.43, 123.00, 54.46, 32.37,

31.74, 29.19, 26.92, 22.56, 14.10. MS (ESI-MS) for $[MNa]^+$, 778.028 (calc.), 778.191 (found). Elemental analysis: Found: C, 79.52; H, 8.25; N, 3.68. Calc. for $C_{50}H_{62}N_2O_4$: C, 79.54; H, 8.28; N, 3.71 %.

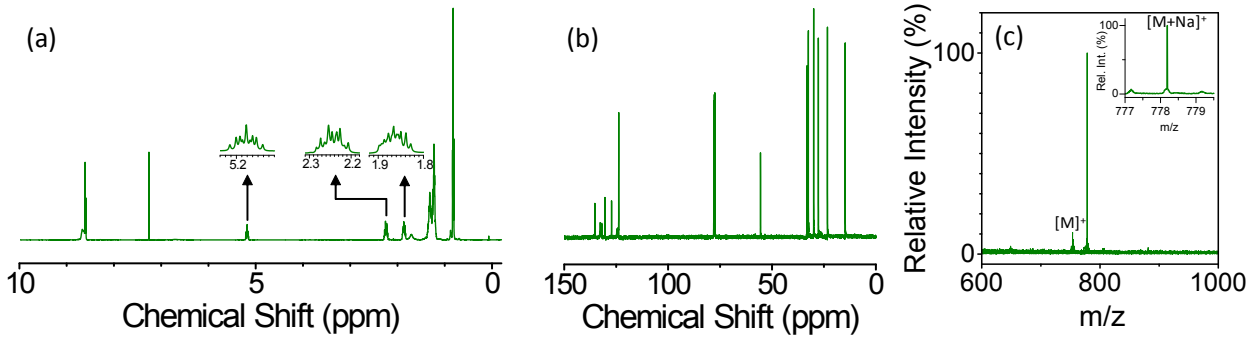

Fig. S5 Characterization of PBI (a) ^{1}H NMR (b) ^{13}C NMR (c) mass spectra (ESI-MS)

III. Self-assembly of the PMMA-*b*-PPEGMA

Self-assembly of the block copolymers was studied by DLS in aqueous medium at 25 °C (Figure S3). The average hydrodynamic diameter (D_h) of P(M_{46}-*b*-P_{24}) was obtained as 34±2 nm. Additionally, D_h for P(M_{46}-*b*-P_{39}) and P(M_{46}-*b*-P_{62}) in aqueous medium were found to be 37±3 and 44±4 nm, respectively, whereas D_h for P(M_{46}-*b*-P_{85}) was below 10 nm indicating no micellization. Thus, the average D_h values of block copolymers were found to increase with increasing *DP* of hydrophilic PPEGMA segment at a constant PMMA block length except the last one. This can be explained as too long hydrophilic block disrupts the amphiphilic balance, essential for self-assembly.

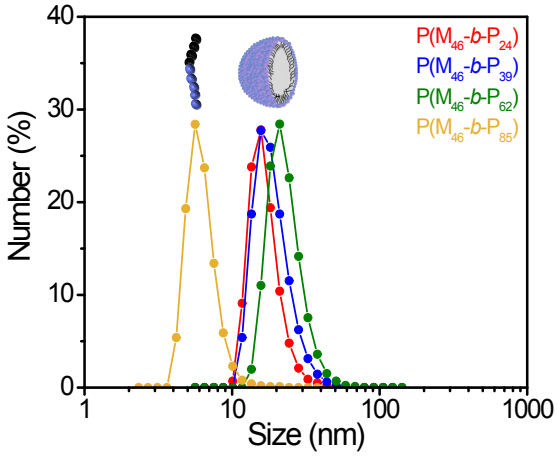

Fig. S6 Size distribution by number of the P(M-*b*-P) block copolymers in aq. medium (1.0 mg/mL) at 25 °C

FE-SEM analysis was also performed to obtain more information about the size and structure of these self-assembled species. Formation of spherical micelles of P(M_{46}-*b*-P_{24}), P(M_{46}-*b*-P_{39}) and P(M_{46}-*b*-P_{62}) in

aqueous solution with size around 20, 38 and 43 nm, respectively were observed in FE-SEM (Figure S4, A-C). Hence FE-SEM data agree with the DLS observation considering the different measurement conditions. FE-SEM micrographs of P(M_{46}-*b*-P_{39}) after dye encapsulation (Fig. S4, D-F) shows retention of micellar assembly.

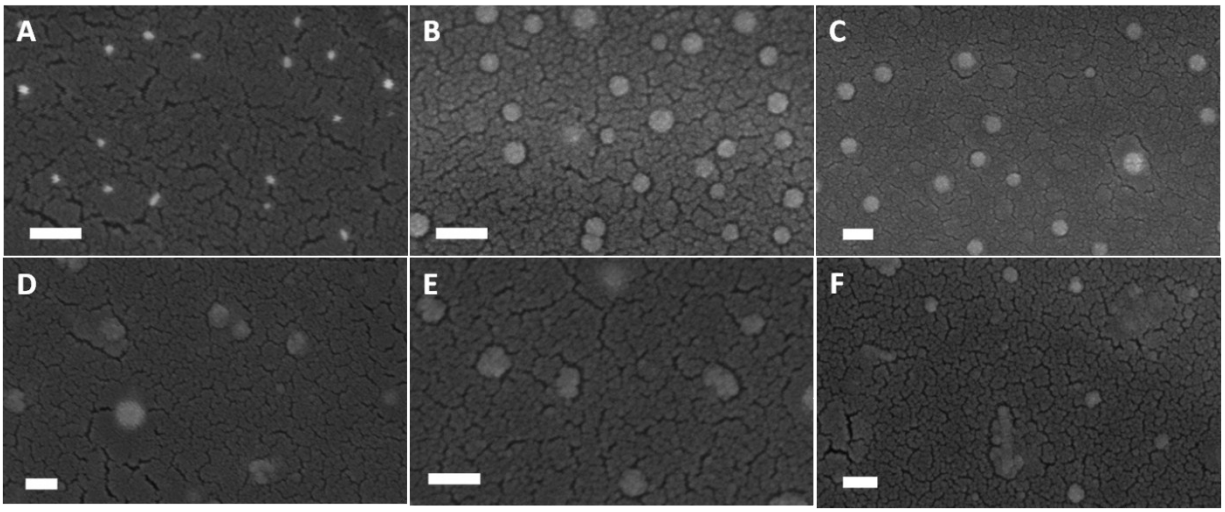

Fig. S7 FE-SEM images of PMMA-*b*-PPEGMA micelle (A) P(M_{46}-*b*-P_{24}); average diameter ~20 nm (B) P(M_{46}-*b*-P_{39}); average diameter ~38nm (C) P(M_{46}-*b*-P_{62}); average diameter ~43 nm. P(M_{46}-*b*-P_{39}) micelle after (D) R-cNDI encapsulation (E) 2R-cNDI encapsulation (F) after R-cNDI and 2R-cNDI co-encapsulation. Scale bar: 100 nm.

IV. Interaction of dyes with its environment

In THF and MCH

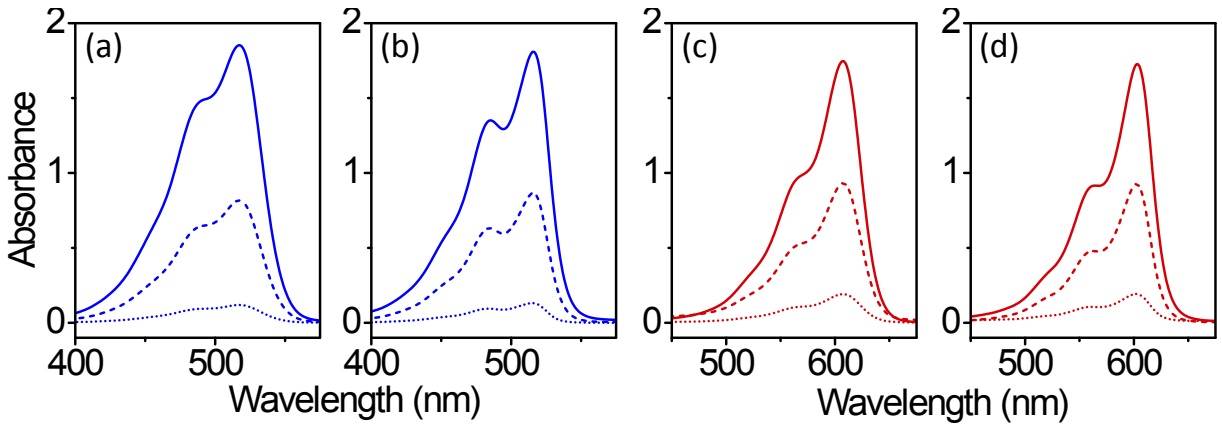

Figure S8. Concentration dependent optical absorption spectra of R-cNDI in (a) THF and (b) MCH, and

2R-cNDI in (c) THF and (d) MCH, respectively. The dye concentrations in each experiment were 16 µg/ml (dotted curves), 80 µg/ml (dashed curves), and 160 µg/ml (solid curves), respectively.

In water

In a control experiment, solutions of R-cNDI and 2R-cNDI in THF (0.6 mg/mL) were mixed with water in 1:37 v/v ratio, filtered through 0.45 μm syringe filter. Optical absorption spectrum of the filtrate shows

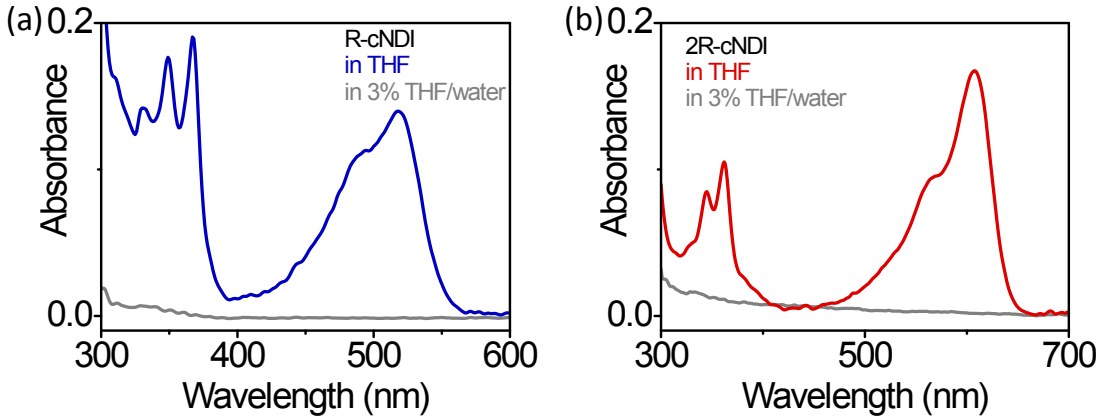

Fig. S9 Optical absorption spectrum of (a) R-cNDI and (b) 2R-cNDI, in THF and in 3% THF in water

no trace of dyes, thereby suggesting a complete precipitation of the dyes in aqueous medium, in absence of polymer micelles.

In aqueous suspension of PMMA-b-PPEGMA micelle

To a solution of PMMA-*b*-PPEGMA in THF (0.2 g/mL), HPLC water was added to bring the copolymer concentration down to 1 mg/mL. The resultant solution mixture was stirred at room temperature for 24 h to evaporate THF and induce micellization. A solution of dye (R-cNDI or 2R-cNDI) in THF (0.6 mg/mL) was added to the above mentioned aqueous suspension of pre-formed PMMA-*b*-PPEGMA micelle in 1:37 v/v ratio, and stirred at 25 °C for 3 days to evaporate THF. The final aqueous suspension had a concentration of 1 mg/mL with respect to the copolymer, and a dye to copolymer ratio of 1:62 w/w. The suspension was filtered through a 0.45 µm syringe filter to remove any insoluble matter, and used for subsequent measurements. Photographs of the filtered solutions indicate retention of hydrophobic dye in the aqueous medium.

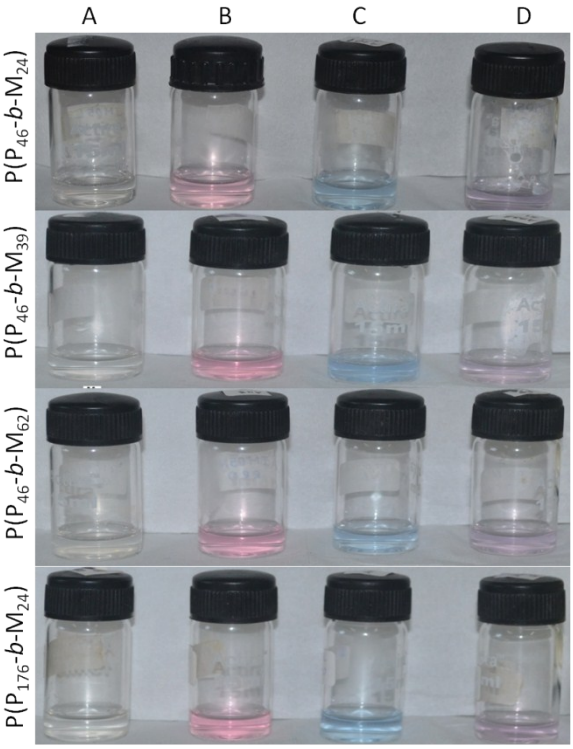

Fig. S10 Retention of dyes in aqueous suspension of different PMMA-*b*-PPEGMA copolymers, after filtration (A) without dye (B) 1:62 w/w R-cNDI to copolymer (C) 1:62 w/w 2R-cNDI to copolymer (D) 1:1:124 R-cNDI to 2R-cNDI to copolymer

Photoluminescence (PL) spectroscopy is consistent with the aggregated state of the dyes. In case of PBI, the vibronically resolved PL spectrum of mono-molecular PBI is replaced by a broad, structureless excimer emission, well known for PBI aggregates. R-cNDI, 2R-cNDI shows a complete PL quenching, as expected for an H-aggregate.

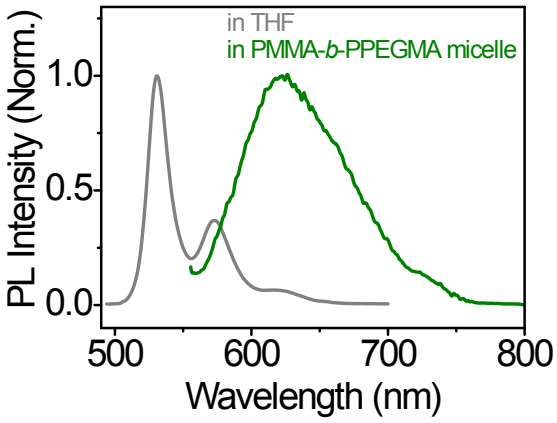

Fig. S11 Normalized PL spectra of PBI in THF (λ_{ex} = 520 nm), and in aqueous suspension of P(M_{46}-*b*-P_{39}) micelle (λ_{ex} = 540 nm).

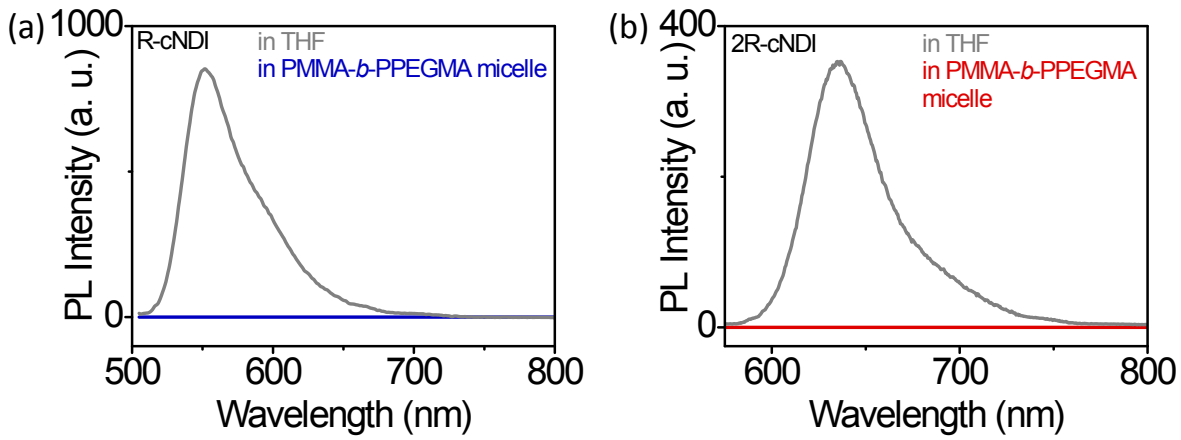

Fig. S12 PL spectra of (a) R-cNDI in THF (grey) and in aqueous suspension (blue) of P(M_{46}-*b*-P_{39}) micelle (λ_{ex} = 494 nm) (b) 2R-cNDI in THF (grey) and in aqueous suspension (red) of P(M_{46}-*b*-P_{39}) micelle (λ_{ex} = 560 nm)

Coencapsulation of R-cNDI and 2R-cNDI in PMMA-b-PPEGMA micelle

To a solution of PMMA-*b*-PPEGMA in THF (0.2 g/mL), HPLC water was added to bring the copolymer concentration down to 1 mg/mL. The resultant solution mixture was stirred at room temperature for 24 h to evaporate THF and induce micellization. An 1:1 w/w solution of R-cNDI and 2R-cNDI in THF (total dye concentration = 0.6 mg/mL) was added to the above mentioned aqueous suspension of pre-formed PMMA-*b*-PPEGMA micelle in 1:37 v/v ratio, and stirred at 25 °C for 3 days to evaporate THF. The final aqueous suspension had a concentration of 1 mg/mL with respect to the copolymer, and dye (RcNDI+2R-cNDI) to copolymer ratio of 1:62 w/w. The suspension was filtered through a 0.45 µm syringe filter to remove any insoluble matter, and used for subsequent measurements.

In PEGMA and hydrated PEGMA

Interaction between hydrophilic PEGMA and cNDI dyes was studied in a solution of dye (16 µg/mL) in 97% PEGMA/THF medium. In order to simulate the encapsulation experiment, where PEGMA block (outer shell of the micelle) is hydrated, 10% v/v water was added to the previous solution, and subsequently filtered with 0.45 μm syringe filter.

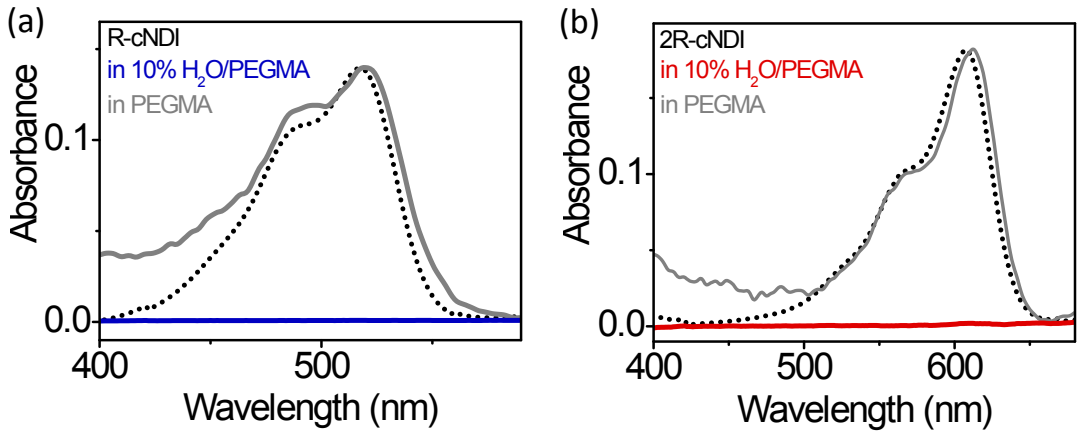

Figure S13. Optical absorption spectra of (a) R-cNDI and (b) 2R-cNDI, dispersed in PEGMA shows an absolute predominance of mono-molecular forms. Dotted black lines present the corresponding spectra in THF. Addition of a small quantity of water (10% v/v) leads to a complete precipitation of both dyes.

In PMMA

PMMA and dye were co-dissolved in $CHCl_3$, such that the final concentration of the dye (R-cNDI or 2R-cNDI) was 0.6 mg/mL and that of PMMA was 100 mg/mL. Optical absorption spectra of the resulting solution, and thin films cast from this solution were measured.

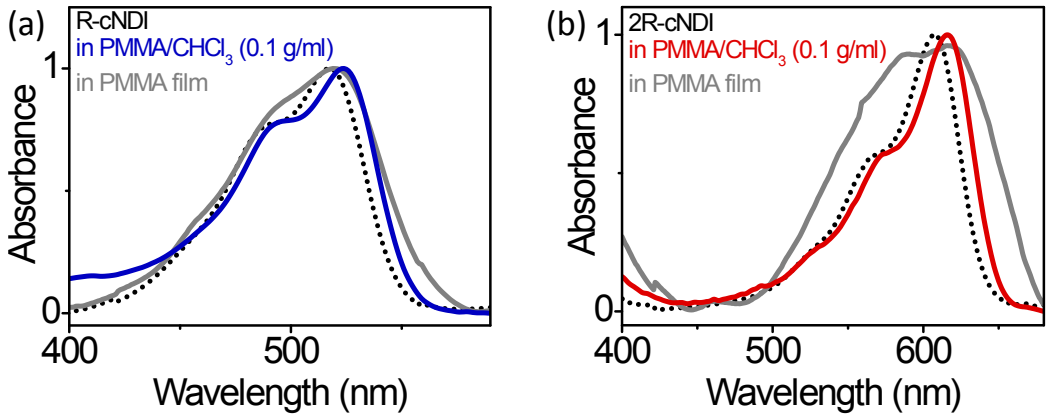

Figure S14. Optical absorption spectra of (a) R-cNDI and (b) 2R-cNDI, dispersed in 100 mg/mL PMMA/$CHCl_3$ solution shows absence of any aggregation. Dotted black lines present the corresponding spectra in THF. Corresponding spectra in solid films show some spectral broadening, but no signs of dye aggregation can be seen.

In un-micellized PMMA-b-PPEGMA

The purpose of this control experiment was to study the effect of molecular interaction between the cNDI dyes and the un-micellized copolymer. Micellization of PMMA-*b*-PPEGMA in water is a slow process that usually takes several hours. In order to preclude micellization, the dye and copolymer were simultaneously dissolved in 3% THF/water, and subsequently filtered through a 0.45 μm syringe filter for further experiments. All other conditions were kept the same as that of the encapsulation experiment.

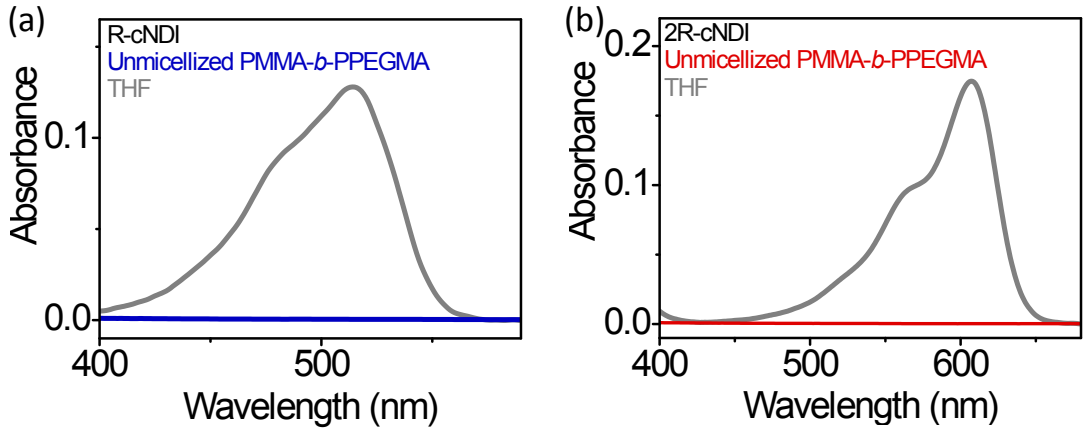

Figure S15. Optical absorption spectra of (a) R-cNDI and (b) 2R-cNDI in a 3% THF/H_2O solution of un-micellized P(M_{46}-*b*-P_{39}) shows a rapid and complete precipitation of the dyes.

V. Transmission Electron Microscopy

We can identify ~40 nm sized spherical micelles with the core and the shell of the micelle exhibiting different contrast before encapsulation (A). Upon encapsulation of 2R-cNDI (B), we notice a marked decrease in the transparency of the core region, which suggest a preferential localization of dye molecules in the hydrophobic core.

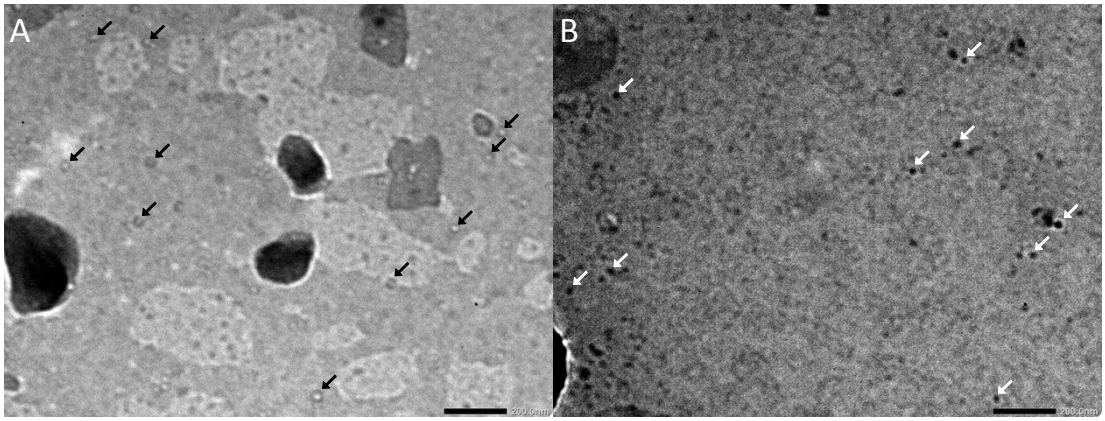

Figure S16. Transmission electron micrographs of the polymer micelles before (A) and after (B) 2R-cNDI encapsulation. Scale bar: 200 nm

VI. Effect of concentration

The effect of dye concentration on the final aggregated state was studied for R-cNDI and 2R-cNDI. The dye concentration was changed from 5-160 µg/ml, while keeping the copolymer P(M_{46}-*b*-P_{39}) concentration fixed at 1 mg/ml.

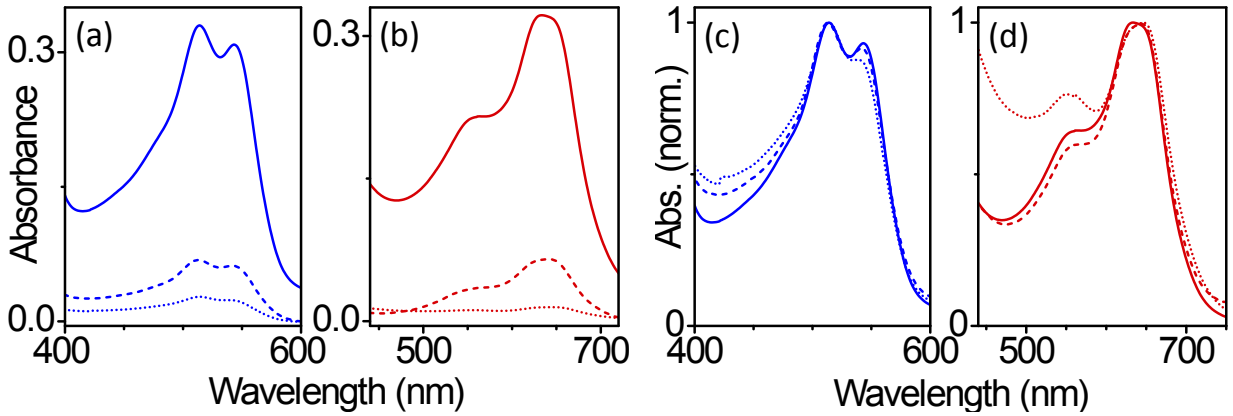

Figure S17. Extent of encapsulation at different concentration. Steady state optical absorption spectra of R-cNDI (blue curves) and 2R-cNDI (red curves) before (a, b) and after (c, d) normalization, respectively. The dye concentrations used were 5 µg/ml (dotted curves), 16 µg/ml (dashed curves), and 160 µg/ml (solid curves), respectively.

The extent of encapsulation scales with the initial concentration of the dye. However upon normalization, spectra at all three concentrations look fairly identical (Fig. S18 c and d). The fact that the

nature and distribution of encapsulated aggregate is independent of the dye concentration indicates that the aggregation pathway is largely controlled by the environment inside the micellar core.

VII. Temperature dependent kinetics

Kinetics of encapsulation induced aggregation of R-cNDI and 2R-cNDI dyes were studied at 20 and 40 °C, for duration of 5 hours, following an exactly identical procedure, as described in the main text. In case of R-cNDI (Fig. S20a and b), the $t_{initial}$ spectrum (black lines) is nearly the same as that at the end of 5 h (blue lines), thereby suggesting that the aggregation of encapsulated dyes is almost instantaneously achieved. The extent of H-aggregation of R-cNDI at 40 °C is lesser than that observed at lower temperatures, as evident from the higher $A_{0\text{-}0}/A_{0\text{-}1}$ ratio.

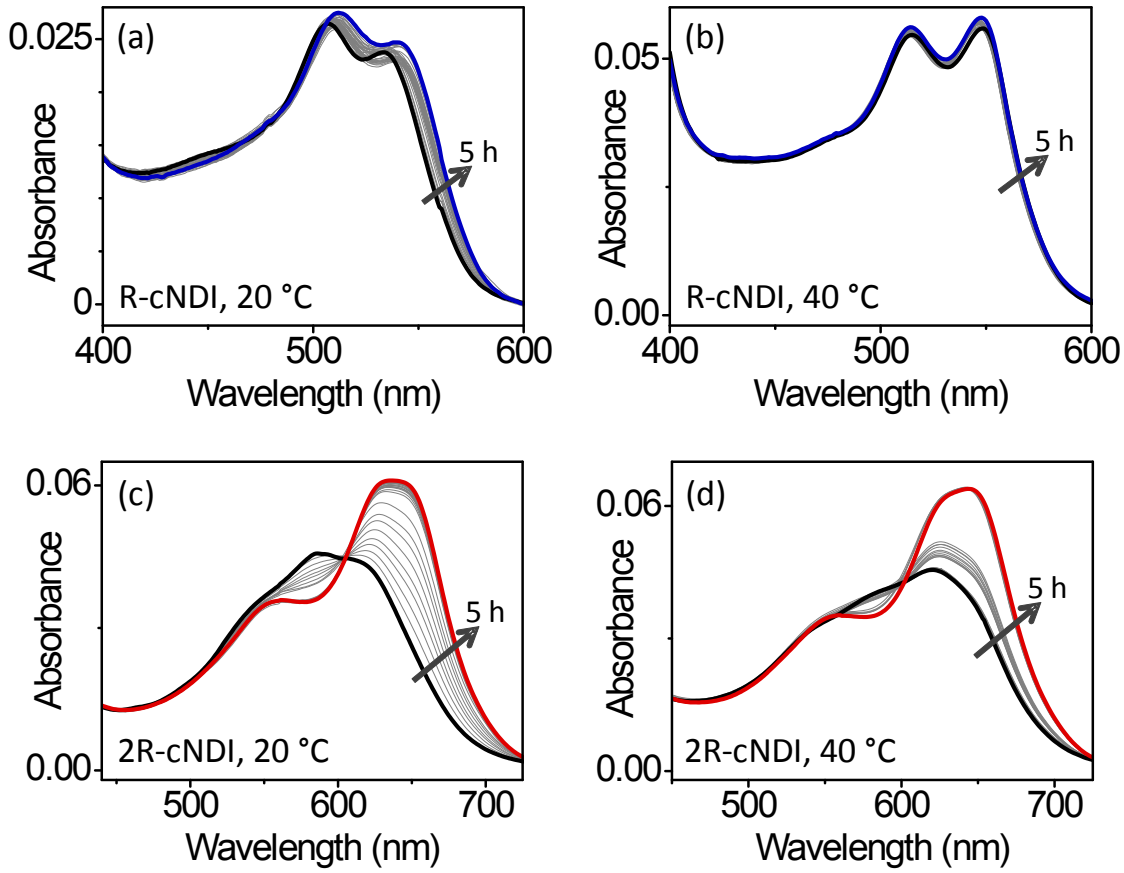

Figure S18. Temperature dependent kinetics of encapsulation induced aggregation of R-cNDI (blue) at (a) 20 °C, and (b) 40 °C, and 2R-cNDI (red) at (c) 20 °C, and (d) 40 °C, over 5 h duration.

Kinetics of encapsulated 2R-cNDI (Fig. S20c and d) reveals a very similar behavior. An instantaneous H-aggregation is evident from the $t_{initial}$ spectrum (black lines). Reorganization from H- to J-aggregate

follows a very similar kinetics, as suggested by the spectra at the end of 5 h (red lines). This weak temperature dependence on the kinetics of aggregation seems to indicate that the micellar core offers an apparent thermal insulation. This point can be further investigated in detail, by studying temperature dependent aggregation of a dye in solution vis-à-vis within the micellar core.

We could not explore a wider temperature range for our kinetic studies because of: (a) limited solubility of the dyes in 1:37 THF/water, below 20 °C, and (b) large variations in the degree of encapsulation at 40 °C and higher.

VIII. H-aggregation of 2R-cNDI

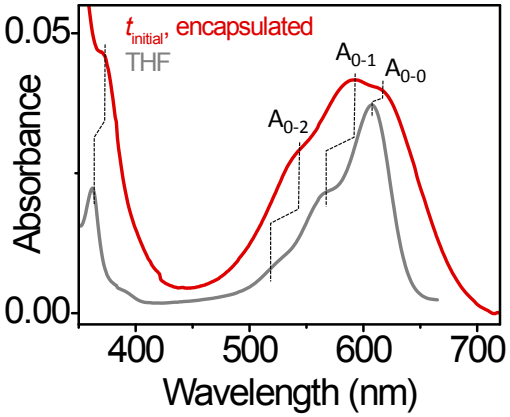

Figure S19. A comparison of $t_{initial}$ absorption spectrum of encapsulated 2R-cNDI with that in THF solution shows the change in A_{0-0}/A_{0-1} ratio, consistent with an H-type aggregation.

IX. Spectral decomposition of time-dependent absorption spectra of 2R-cNDI

The time dependent absorption spectral series of encapsulated 2R-cNDI shows a distinct isosbestic point at 601 nm, which strongly favours the *two species* model: the initial H-aggregate and the *reorganized aggregate*. Consequently, we express the experimental absorption spectrum $S_{\mathrm{exp}}(t)$ as a time-dependent linear combination:

$$S_{exp}(t) = a_H(t)\, S_H + \{1 - a_H(t)\}\, S_R$$, where

S_{H} and S_{R} denote the absorption spectra of the H- and the reorganized aggregate, respectively. Similarly, $a_{\mathrm{H}}(t)$ and $\{1 - a_{\mathrm{H}}(t)\}$ are the time-dependent fractions of the H- and the reorganized aggregates, respectively. Since, H-aggregates are formed exclusively after encapsulation, we assume S_{H}

$= S_{\text{exp}}(t_{\text{initial}})$ with a high degree of certainty. The spectrum of the reorganized aggregate, S_{R} at each time t is therefore calculated as,

$$S_R = \frac{S_{exp}(t) - a_H(t)\, S_{exp}(t_{initial})}{1 - a_H(t)},$$

The only restriction imposed is on the value of $a_{\text{H}}(t)$, such that $S_{\text{R}} \geq 0$ over the entire wavelength range.

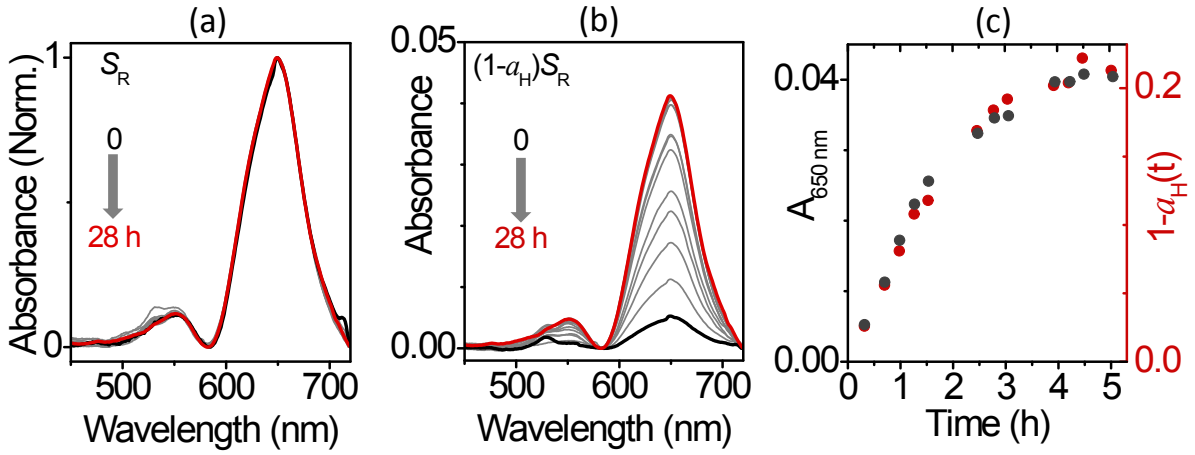

Figure S20. (a) S_{R}, calculated from the spectral decomposition of different $S_{\text{exp}}(t)$ over a span of 28 hours, and normalized for comparison, resemble each other perfectly well, (b) S_{R} weighted with the time-dependent relative fraction, 1-$a_{\text{H}}(t)$. (c) Fraction of the reorganized aggregate, calculated from the spectral decomposition (1-a_{H}) and experimentally obtained from the absorbance at 650 nm (A_{650}) shows an identical time-dependence.

X. Thermal stability of encapsulated aggregates

Temperature dependent absorption spectroscopy offers a convenient method to investigate the mechanism of supramolecular aggregation, and is particularly useful in cases where multiple aggregation pathways are operative. An aqueous suspension of encapsulated 2R-cNDI at steady state (16 µg/ml, 25 °C) was cycled between 25 and 60 °C and back, under thermodynamic control (at 0.15 °C/min). Fig. S19a and b show the temperature dependent absorption spectra for heating and cooling runs, respectively. Upon heating, the dominant J-type band shows a gradual blue shift (~7 nm), and merges with the absorption feature of H-aggregate at higher temperatures. This effect is completely reversible, as cooling down to 25 °C (at 5 °C/min rate) regains the original spectrum. Spectral decomposition of absorption spectra at 25 and 60 °C (Fig. S19 c and d, respectively) show the relative contributions of H- and J- type aggregates to be very similar (within ~10%). It is remarkable that no

aggregate dissociation is observed at higher temperatures. This is a surprising result considering the fact that aggregates of several strongly pi-stacking perylene bisimide undergo significant disassembly at 60 °C.[4] This apparent thermal insulation provided by the micellar encapsulation is also seen in our kinetic experiments.

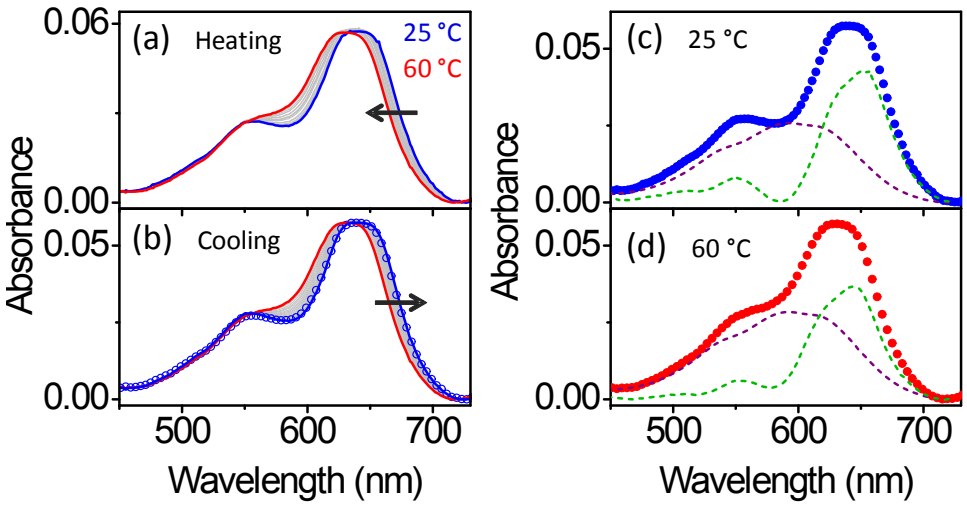

Figure S21. Temperature dependent absorption spectroscopy of encapsulated 2R-cNDI aggregates (16 µg/ml) during (a) heating and (b) cooling runs, at a rate of 0.15 °C/min. Comparing the spectra at 25 °C at the beginning of heating (blue line) and end of cooling run (blue open circles) shows that the effect of temperature is fully reversible. Spectral decomposition of the absorption spectra at (b) 25 °C, and (c) 60 °C, reveal relative contributions of the H-(purple dashed line) and J-aggregated species (green dashed line) to be very similar at 25 and 60 °C. The spectrum of the J-aggregated species blue-shifts gradually upon heating, with an overall shift of 7 nm at 60 °C.

XI. References

1. J. Ferguson, R. J. Hughes, B. T. T. Pham, B. S. Hawkett, R. G. Gilbert, A. K. Serelis and C. H. Such, *Macromolecules*, 2002, **35**, 9243–9245.

2. M. Sasikumar, Y. V. Suseela, T. Govindaraju, *Asian J. Org. Chem.*, 2013, **2**, 779.

3. C. Lu, M. Fujitsuka, A. Sugimoto, and T. Majima, *J. Phys. Chem. C,* 2016, **120**, 12734.

4. S. Ogi, V. Stepanenko, K. Sugiyasu, M. Takeuchi, and F. Würthner, *J. Am. Chem. Soc.*, 2015, **137**, 3300; C. Kulkarni, K. K. Bejagam, S. P. Senanayak, K. S. Narayan, S. Balasubramanian, and S. J. George, *J. Am. Chem. Soc.*, 2015, **137**, 3924; F. Würthner, T. E. Kaiser, and C. R. Saha-Möller, *Angew. Chem. Int. Ed.*, 2011, **50**, 3376